Differential detection of correlative encoded continuous phase modulation schemes using decision feedback

Dimitrios Makrakis, PhD
Prof. P. Takis Mathiopoulos, PhD

Indexing terms: Detection, Phase modulation, Receivers

Abstract: We generalise a differential detection technique, introduced elsewhere for a Gaussian minimum shift keying (GMSK) scheme, to include any correlative encoded continuous phase modulated (CECPM) signalling format. The proposed symbol-by-symbol receivers employ decision feedback to partially remove the effects of the destructive intersymbol interference (ISI) which corrupts the differentially detected CECPM signal. After achieving wider eye opening with the decision feedback, the outputs of the two or more differential detectors are jointly utilised to further improve the performance. As a typical example of the CECPM family of signals and because of its excellent spectral characteristics, the new receiver configurations employing up to 3-bit differential detectors have been applied to a tamed frequency modulation (TEM) signal. Bit error rate (BER) performance evaluation results have indicated that performance improvements of more than 5 dB (at BER = 10^{-4}) over a conventionally differential detected TFM scheme are possible. As compared with a limiter/discriminator receiver employing maximum likelihood sequence estimation (MLSE), the proposed receivers offer gains of more than 2 dB (at BER = 10^{-4}).

1 Introduction

In a recent paper [1], a new detection technique based on decision feedback and signal combining, which improves the performance of differential detected GMSK schemes, has been introduced. GMSK belongs to the family of CECPM signals, which have well known attractive properties such as constant envelope and compact spectrum [2, 3]. Examples of other popular CECPM signals include partial response continuous phase modulation (PRCPM) [4], correlative phase shift keying (CPSK) [5], duobinary frequency shift keying (DFSK) [6], tamed frequency modulation (TFM) [7] and generalized TFM (GTFM) [8].

Paper 8144I (E7, E8), first received 6th November 1990 and in revised form 11th April 1991

Dr. Makrakis is with the Communication Research Centre, PO Box 11490, Station H, Ottawa, Ontario, Canada K2H 8S2

Prof. Mathiopoulos is with the Department of Electrical Engineering, University of British Columbia, Vancouver, BC, Canada V6T 1Z4

Correspondence should be addressed to Prof. Mathiopoulos

Since the various CECPM schemes have advantages and disadvantages, the choice of signal depends on the particular application. In general the tradeoffs considered are narrow power spectrum, low out-of-band energy, better bit error rate (BER) performance, and low overall implementation complexity [9].

Motivated by the performance improvements of the detection technique reported in [1], in this paper we present its generalisation so that any CECPM scheme employing differential detection can be accommodated. As an example, we apply the proposed generalised technique to improve the performance of a differentially detected TFM signal.

2 *m*-Bit differential detection of CECPM schemes

The block diagram of the system under consideration is given in Fig. 1. Its transmitter consists of a differential encoder (DE), a correlative encoder (CE), a premodulation lowpass filter (LPF), which has an impulse response $h(t)$, and an FM modulator with a modulation index $m_h = 0.5$. The DE is optional, and its presence and structure depend on the particular CECPM scheme as well as on the differential receiver to be employed. When the DE is not used, $a_k = b_k$. The a_ks are equiprobable binary random variables taking values from the alphabet $\{\pm 1\}$. The CE is described by the following system polynomial [10]:

$$F(D) = \frac{1}{D_{en}} \sum_{j=-1}^{n} g_j D^j \tag{1}$$

where D is the delay operator corresponding to a T second delay [10], and

$$D_{en} = \sum_{j=-l}^{n} g_j \tag{2}$$

In eqn. 2 the g_js represent the coefficients of the correlative encoder, and l, n are integers greater than or equal to zero. Furthermore, it will be assumed that the LPF, $h(t)$, satisfies the following relation:

$$\int_{kT-T}^{kT} h(\tau)\, d\tau = \begin{cases} 1/2 & \text{if } k = 0 \\ 0 & \text{otherwise} \end{cases} \tag{3}$$

The input to the CE is a sequence of impulses, i.e.

$$b(t) = \sum_{k=-\infty}^{\infty} b_k \delta(t - kT) \tag{4}$$

where T is the symbol duration. The output of the LPF can be expressed as

$$s(t) = \sum_{k=-\infty}^{\infty} c_k h(t - kT) \tag{5}$$

with c_k given by

$$c_k = \frac{1}{D_{en}} \sum_{j=-1}^{n} b_{k-j} g_j \tag{6}$$

an m-bit differential detector. In general, the output of the m-bit differential detector, $d_m(t)$, is obtained by lowpass filtering the product $y(t)$ with an mT delayed and θ_m phase-shifted version of itself, i.e.

$$d_m(t) = r(t)r(t - mT) \cos \left[2\pi m_h \times \sum_{j=-\infty}^{\infty} c_j \int_{t-mT}^{t} h(\tau - jT)\, d\tau - \theta_m \right] + n_m(t) \tag{10}$$

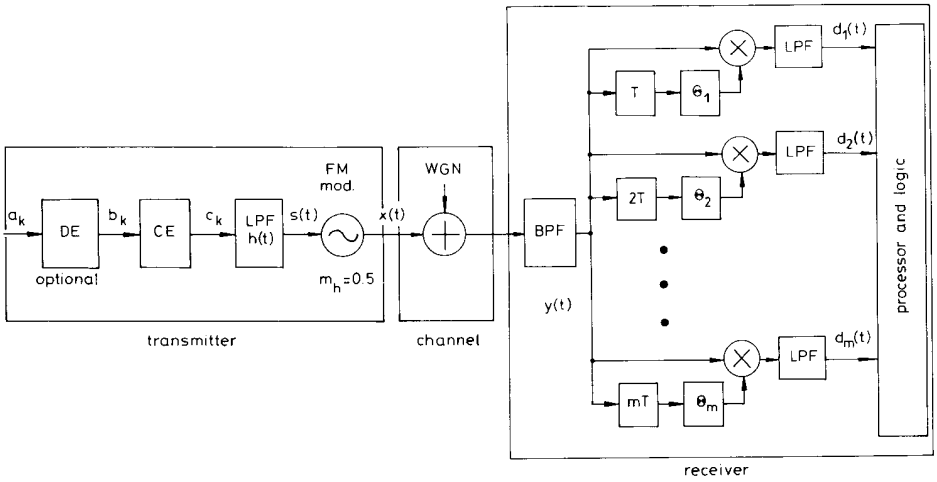

Fig. 1 *Block diagram of the system under consideration*

Finally, the output of the FM modulator is the following signal:

$$x(t) = A_0 \cos [\omega_c t + \phi(t) + \psi] \tag{7}$$

In the above equation, A_0 is the envelope of the transmitted signal, ω_c is the carrier radian frequency, ψ is the initial phase of the modulator, and $\phi(t)$ is the information carrying phase, which is given by

$$\phi(t) = 2\pi m_h \int_{-\infty}^{t} s(\tau)\, d\tau = 2\pi m_h \sum_{j=-\infty}^{\infty} c_j \int_{-\infty}^{t} h(\tau - jT)\, d\tau \tag{8}$$

where m_h is the modulation index and equals 0.5. It should be mentioned that, without any loss of generality, in eqn. 7 A_0 will be assumed to be equal to one and ψ equal to zero.

$x(t)$ is corrupted by additive white Gaussian noise (AWGN) with a one-sided power spectral density of N_0. The signal at the output of the roofing bandpass filter (BPF) can then be represented as

$$y(t) = r(t) \cos [\omega_c t + \phi'(t)] + n_{bp}(t) \tag{9}$$

where $\phi'(t)$ is the distorted signal phase, $r(t)$ is the time-varying envelope of the signal and $n_{bp}(t)$ is the narrowband Gaussian noise. In order to simplify the mathematical analysis, we shall assume that $\phi'(t) = \phi(t)$; however, in the computer simulations the distortion due to filtering is included.

As shown in Fig. 1, the receiver consists of a bank of multiple differential detectors of maximum order m, i.e. the maximum delay element is mT, which corresponds to

where

$$\theta_m = \begin{cases} 90° & \text{for } m \text{ odd} \\ 0° & \text{for } m \text{ even} \end{cases} \tag{11}$$

and $n_m(t)$ represents the baseband noise terms. At $t = kT$, $d_m(t)$ becomes

$$d_m(kT) = r(kT)r(kT - mT) \times \cos \left(\sum_{j=-\infty}^{\infty} c_j V_{k-j}^m - \theta_m \right) + n_m(kT) \tag{12}$$

where

$$V_{k-j}^m = 2\pi m_h \int_{kT-mT}^{kT} h(\tau - jT)\, d\tau \tag{13}$$

Using eqns. 3 and 13 we find that

$$V_k^m = \begin{cases} \pi m_h & \text{for } k > 0 \text{ and } k \leqslant m \\ 0 & \text{otherwise} \end{cases} \tag{14}$$

Eqn. 6 enables us to write eqn. 12 in the form

$$d_m(kT) = r(kT)r(kT - mT) \times \cos (\Delta U_k^m - \theta_m) + n_m(kT) \tag{15}$$

where

$$\Delta U_k^m = \sum_{j=-\infty}^{\infty} b_{k-j} U_j^m \tag{16}$$

$$U_j^m = \frac{1}{D_{en}} \sum_{i=-1}^{n} g_i V_{j-i}^m \tag{17}$$

For the 1-bit differential detector ($m = 1$) we have

$$\Delta U_k^1 = \frac{\pi}{2D_{en}} \sum_{j=-l}^{n} g_j b_{k-j} \tag{18}$$

Similarly, for the 2-bit differential detector ($m = 2$) we get

$$\Delta U_k^2 = \frac{\pi}{2D_{en}} \left[b_{k-n-1} g_n + \sum_{j=1-l}^{n} b_{k-j}(g_j + g_{j-1}) + b_{k+l} g_{-l} \right] \tag{19}$$

For the more general case where $m \geqslant 3$ and $n + l + 1 \geqslant m$, eqn. 16 becomes

$$\Delta U_k^m = \frac{\pi}{2D_{en}} \sum_{j=-l}^{m-l} b_{k-j} \left(\sum_{i}^{l+j} g_{l+i} \right) + \frac{\pi}{2D_{en}} \sum_{j=m-l}^{n-1} b_{k-j} \left(\sum_{i=0}^{m} g_{j-i} \right) + \frac{\pi}{2D_{en}} \sum_{j=n}^{n+m} b_{b-j} \left(\sum_{i=0}^{n+m+i} g_{n-i} \right) \tag{20}$$

Finally, for the case where the order of the differential detector is greater than the memory introduced by the correlative encoder, i.e. $m > n + 1$, we have

$$\Delta U_k^m = \frac{\pi}{2D_{en}} \sum_{j=-l}^{n-1} b_{b-j} \left(\sum_{i=0}^{l+j} g_{-l+i} \right) + \frac{\pi}{2} \sum_{j=n}^{m-l} b_{k-j} + \frac{\pi}{2D_{en}} \sum_{j=m-l}^{n+m} b_{k-j} \left(\sum_{i=0}^{n+m+l} g_{n-i} \right) \tag{21}$$

Eqns. 18–21 provide the mathematical expressions for the differential phase (at the time instant kT) at the output of an mth-order differential detector. As these equations are general enough to accommodate any CECPM signal, they are inevitably complex. However, it should be pointed out that by employing a specific CECPM signal, these expressions will become considerably simplified. This will also be demonstrated in the next section.

3 Application to TFM schemes

Among the great variety of signals belonging to the CECPM family, TFM is a typical example. Because of its compact spectrum, TFM and other narrowband constant envelope digital modulation methods have been proposed to meet the stringent requirements on bandwidth utilisation for future communication services [8]. Thus in this paper we have chosen to analyse TFM as a typical example of a CECPM signal. Nevertheless, it should be noted that the proposed differential detection technique described in this and the subsequent sections can be applied in a relatively straightforward manner to any other member of the CECPM family of signals.

For a TFM signal, we have in eqn. 2 $l = 1$, $n = 1$, $g_1 = g_{-1} = 0.25$ and $g_0 = 0.5$. Substituting these values into eqns. 18–21 we obtain the following expressions:
For $m = 1$ (1-bit differential detector):

$$\Delta U_k^1 = b_{k+1} \frac{\pi}{8} + b_k \frac{\pi}{4} + b_{k-1} \frac{\pi}{8} \tag{22}$$

For $m = 2$ (2-bit differential detector):

$$\Delta U_k^2 = b_{k+1} \frac{\pi}{8} + b_k \frac{3\pi}{8} + b_{k-1} \frac{3\pi}{8} + b_{k-2} \frac{\pi}{8} \tag{23}$$

For $m \geqslant 3$ (3-bit or higher differential detector):

$$\Delta U_k^m = b_{k+1} \frac{\pi}{8} + b_k \frac{3\pi}{8} + \sum_{j=1}^{m-2} b_{k-j} \frac{\pi}{2} + b_{k-m+1} \frac{3\pi}{8} + b_{k-m} \frac{\pi}{8} \tag{24}$$

In the next section we shall briefly describe the operation of the conventional 1-, 2- and 3-bit differential detection of TFM signals. Since the basic principles are the same as in [1], only the end result will be given here.

The output of the 1-bit differential detector can be expressed as

$$d_1(kT) = r(kT)r(kT - T) \sin(\Delta U_k^1) + n_1(kT) \tag{25}$$

Similar to [1] and by using this equation, the differential phase angles ΔU_k^1 which correspond to all possible input data combinations have been calculated and are given in Table 1. In Fig. 2 we also illustrate the equivalent phase-state diagram. It is interesting to notice that when the bit combination $\{b_{k-1}, b_k, b_{k+1}\}$ takes the values $\{-1, 1, -1\}$ or $\{1, -1, 1\}$, the differential phase angle is zero. Therefore in this case the detector cannot distinguish between positive and negative values of b_k. This results in a completely closed eye and makes symbol-by-symbol detection, when using this conventional 1-bit differential detector, impossible.

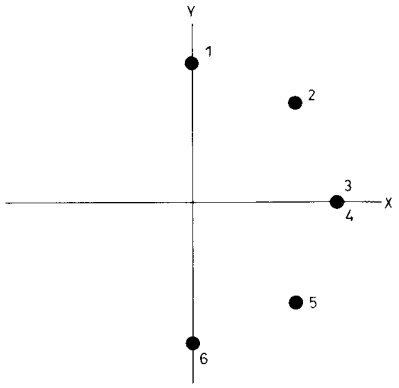

Fig. 2 *Differential phase angles (phase states) ΔU_k^1 of conventional 1-bit differential detector of TFM*

Since states 3 and 4 coincide (i.e. their differential phase angle is zero) conventional symbol-by-symbol detection is not possible and thus there is no decision threshold indicated

Table 1: Differential phase angles (phase states) ΔU_k^1 of the 1-bit differential detector of TFM corresponding to the various combinations of the input data (see also Fig. 2 for equivalent geometrical representations of ΔU_k^1)

Bit combinations			State	ΔU_k^1 (degrees)
b_{k-1}	b_k	b_{k+1}		
1	1	1	1	90.0
1	1	−1	2	45.0
−1	1	1	2	45.0
−1	1	−1	3	0.0
1	−1	1	4	0.0
1	−1	−1	5	−45.0
−1	−1	1	5	−45.0
−1	−1	−1	6	−90.0

For the 2-bit differential detector, the output is given by

$$d_2(kT) = r(kT)r(kT - 2T) \cos(\Delta U_k^2) + n_2(kT) \tag{26}$$

For this detector, the differential phase angles ΔU_k^2 are given in Table 2, and the corresponding phase-state diagram is illustrated in Fig. 3. Clearly, in this case the minimum phase difference between states with opposite polarity of the bits $\{b_{k-2}, b_{k-1}, b_k, b_{k+1}\}$, i.e. states 14

Table 2: Differential phase angles (phase states) ΔU_k^2 of the 2-bit differential detector of TFM corresponding to the various input data combinations (see also Fig. 3 for equivalent geometric representations of ΔU_k^2)

Bit combinations				State	ΔU_k^2 (degrees)
b_{k-2}	b_{k-1}	b_k	b_{k+1}		
1	1	−1	1	7	45.0
1	−1	1	1	7	45.0
1	1	−1	−1	8	0.0
1	−1	1	−1	8	0.0
−1	1	−1	1	8	0.0
−1	−1	1	1	8	0.0
−1	1	−1	−1	9	−45.0
−1	−1	1	−1	9	−45.0
1	−1	−1	1	10	−90.0
1	−1	−1	−1	11	−135.0
−1	−1	−1	1	11	−135.0
−1	−1	−1	−1	12	−180.0
1	1	1	1	12	180.0
1	1	1	−1	13	135.0
−1	1	1	1	13	135.0
−1	1	1	−1	14	90.0

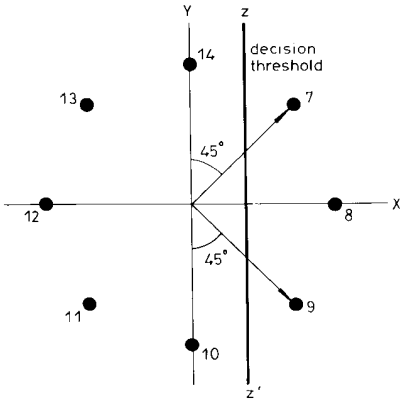

Fig. 3 *Differential phase angles (phase states) ΔU_k^2 of conventional 2-bit differential detector of TFM*

The decision rule for this detector is $\hat{a}_k = \text{sgn}\,[d_2(kT) - (\sqrt{(2)}/4]$, assuming that the states are located on a unity circle

and 7 or 10 and 9, is 45°. To determine the polarity of the decoded bit, the decision threshold zz' illustrated in Fig. 3 will be considered. When the differential phase angle ΔU_k^2 is to the right of zz' (i.e. $-\pi/4 \leqslant \Delta U_k^2 \leqslant \pi/4$), then from Table 2 it can be seen that $b_k b_{k-1} = -1$. (Notice that since a 2-bit differential detector is considered here, only b_k and b_{k-1} will influence the detection process at $t = kT$.) Otherwise we have $b_k b_{k-1} = 1$. Similarly to [1], when a 2-bit differential detector is used, a DE with an output $b_k = -a_k b_{k-1}$ is needed. This differential encoding operation is necessary so that the decisions made at the receiver represent decisions on the true input data sequence (in this case $\{a_k\}$) and not a differentially decoded version of it, as would be the case without the differential encoder at the transmitter [11, 12]. Equivalently, this differential encoding can eliminate error propagations. To see this, assume that the DE is absent, i.e. $a_k = b_k$. Then the estimate of b_k, denoted $\hat{b}_k$, can be determined by using the already decoded $\hat{b}_{k-1}$. However, with this approach an error in $\hat{b}_{k-1}$ will result in erroneous decisions for the subsequent bits. A differential encoder with an output $b_k = -a_k b_{k-1}$ will correct this error propagation because the detection at the output of the differential detector is based upon the rule $a_k = -b_k b_{k-1}$. Thus the decision rule for this detector, assuming that the states in Fig. 3 are located on the unity circle, is given by

$$\hat{a}_k = \text{sgn}\left[d_2(kT) - \frac{\sqrt{(2)}}{4}\right]$$

where sgn $[\cdot]$ is the signum function.

Finally, the output of the 3-bit differential detector is given by

$$d_3(kT) = r(kT)r(kT - 3T)\sin(\Delta U_k^3) + n_3(kT) \qquad (27)$$

The differential phase angles ΔU_k^3 corresponding to all combinations of b_{k-3}, b_{k-2}, b_{k-1}, b_k, b_{k+1} are given in Table 3, and the equivalent state-space diagram is shown

Table 3: Differential phase angles (phase states) ΔU_k^3 of the 3-bit differential detector of TFM corresponding to the various combinations of the input data (see also Fig. 4 for equivalent geometrical representations of ΔU_k^3)

Bit combinations					State	ΔU_k^3 (degrees)
b_{k-3}	b_{k-2}	b_{k-1}	b_k	b_{k+1}		
1	−1	−1	−1	1	15	180.0
1	1	1	−1	1	16	135.0
1	−1	1	1	1	16	135.0
1	−1	−1	−1	−1	16	135.0
−1	−1	−1	−1	1	16	135.0
1	1	−1	1	1	17	90.0
−1	−1	−1	−1	−1	17	90.0
1	1	1	−1	−1	17	90.0
1	−1	1	1	−1	17	90.0
−1	1	1	−1	1	17	90.0
−1	−1	1	1	1	17	90.0
1	1	−1	1	−1	18	45.0
−1	1	−1	1	1	18	45.0
−1	1	1	−1	−1	18	45.0
−1	−1	1	1	−1	18	45.0
−1	1	−1	1	−1	19	0.0
1	−1	1	−1	1	20	0.0
1	1	−1	−1	1	21	−45.0
1	−1	−1	1	1	21	−45.0
1	−1	1	−1	−1	21	−45.0
−1	−1	1	−1	1	21	−45.0
1	1	−1	−1	−1	22	−90.0
1	−1	−1	1	−1	22	−90.0
−1	1	−1	−1	1	22	−90.0
−1	−1	−1	1	1	22	−90.0
1	1	1	1	1	22	−90.0
−1	−1	1	−1	−1	22	−90.0
1	1	1	1	−1	23	−135.0
−1	−1	−1	1	−1	23	−135.0
−1	1	1	1	1	23	−135.0
−1	1	−1	−1	−1	23	−135.0
−1	1	1	1	−1	24	−180.0

in Fig. 4. ΔU_k^3 is positive when $b_k b_{k-1} b_{k-2}$ is -1, whereas ΔU_k^3 is negative when $b_k b_{k-1} b_{k-2}$ is 1. Thus for the 3-bit differential detector, in order to avoid error propagation the data should be differentially encoded as $b_k = -a_k b_{k-1} b_{k-2}$. Clearly with this encoding law we have $a_k = -b_k b_{k-1} b_{k-2}$, and therefore whenever $a_k = 1$ then $0 \leqslant \Delta U_k^3 \leqslant \pi$, and whenever $a_k = -1$ then $-\pi \leqslant \Delta U_k^3 \leqslant 0$. Notice, however, that states 15 and 19 ($b_k = 1$) and states 20 and 24 ($b_k = -1$) lie on the same X-axis, so that the eye of the 3-bit differential detector is completely closed.

Examining detectors with $m > 3$ we found that:

(*a*) For m odd the eye diagram is completely closed.

(*b*) For m even, the eye is asymmetric and open. However, the eye is always the same as that of the 2-bit detector. For $m \geq 2$ a differential decoder is needed to avoid catastrophic error propagation. This differential

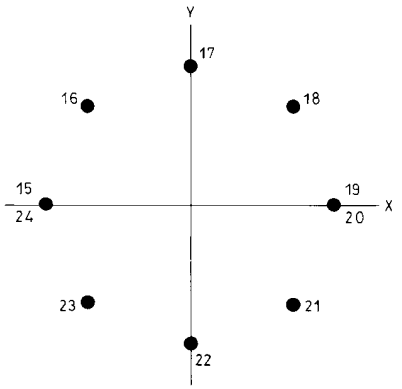

Fig. 4 *Differential phase angles (phase states) ΔU_k^3 of conventional 3-bit differential detector of TFM*

Similarly to the 1-bit detector, since states 15 and 19 coincide with states 24 and 20, conventional symbol-by-symbol detection is not possible and thus there is no decision threshold indicated

decoder becomes more complex with increasing m, and at the same time the performance of the detector does not exceed the performance of the 2-bit detector.

In concluding this section we can state that the best choice for conventional differential detection of TFM is the 2-bit detector.

4 ISI reduction by means of decision feedback

In order to reduce the effects of the ISI, which, as shown in the previous section, is present in the differential detection of TFM signals, a decision feedback technique similar to that suggested in [1] will be employed. It should be mentioned that although we will present results only for TFM signals, the application of the proposed technique to any other CECPM scheme is straightforward. For this purpose, we include the general forms of equations for this decision feedback technique; however, whenever possible extensive mathematical manipulations have been avoided.

4.1 Decision feedback for the 1-bit differential detector

For the 1-bit differential detection of TFM, at the instant $t = kT$, ΔU_k^1 depends on b_k, b_{k-1} and b_{k+1} (see eqn. 22). When b_k is to be decided, the estimate of b_{k-1}, which will be denoted $\hat{b}_{k-1}$, is already available. Hence by introducing the new phase shift χ_1, which includes the phase $\theta_1 = \pi/2$ (see eqn. 11) and is given by

$$\chi_1 = \frac{\pi}{2} + \hat{b}_{k-1} U_1^1 = \frac{\pi}{2} + \hat{b}_{k-1} \frac{\pi}{8} \tag{28}$$

in the T second delay arm, the effect of b_{k-1} on the signal phase can be cancelled. The new differential phase angle $\Delta U_{k,d}^1$ becomes

$$\Delta U_{k,d}^1 = b_{k+1} U_{-1}^1 + b_k U_0^1 = b_{k+1} \frac{\pi}{8} + b_k \frac{\pi}{4} \tag{29}$$

For states 3 and 4, the effects of b_{k-1} are always destructive since $b_k \neq b_{k-1}$. A phase shift equal to $\hat{b}_{k-1} U_1^1$ will increase the distance from the decision threshold (i.e. X-axis) by an angle $U_1^1 = \pi/8$. For states 2 and 5, the effect of b_{k-1} can be constructive or destructive. If $b_k \neq b_{k-1}$, its effect is destructive and the application of decision feedback increases the differential phase by $\pi/8$. On the other hand, when $b_k = b_{k-1}$ the decision feedback reduces the differential phase by $\pi/8$.

States 1 and 6, which have the widest separation, always have $b_k = b_{k-1}$, and the application of decision feedback reduces the differential phase angle by $\pi/8$. However, notice that in terms of the system performance the critical states are 3 and 4. Hence the reduction of $\Delta U_{k,d}^1$ for states 1, 2, 5 and 6 is several times compensated by its equivalent increase for states 3 and 4.

The phase states at the sampling instants, after applying decision feedback, are shown in Fig. 5. It is clear from this figure that there is a $\pi/4$ rad phase separation

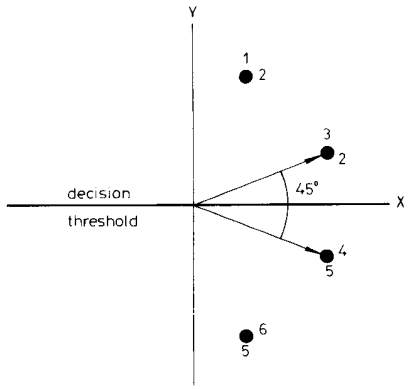

Fig. 5 *Phase-state diagram of the 1-bit differential detector of TFM with decision feedback*

The decision rule for this detector is $\hat{a}_k = \text{sgn}\,[d_1'(kT)]$

between the states closest to the threshold (X-axis). The decision rule for this detector is

$$\hat{b}_k = \text{sgn}\,[d_1'(kT)]$$

where $d_1'(kT)$ denotes the equivalent signal $d_1(kT)$ which includes the additional phase shift χ_1. Notice that for the 1-bit differential detector no differential encoding is needed and thus $a_k = b_k$.

4.2 Decision feedback for the 2-bit differential detector

For the 2-bit differential detector, there are four symbols that introduce ISI at ΔU_k^2. These are b_{k+1}, b_k, b_{k-1} and b_{k-2}. By introducing at the $2T$ delay arm a phase shift equal to

$$\chi_2' = \hat{b}_{k-1} U_1^2 + \hat{b}_{k-2} U_2^2 = \hat{b}_{k-1} \frac{3\pi}{8} + \hat{b}_{k-2} \frac{\pi}{8} \tag{30}$$

where $\hat{b}_{k-2}$ is the estimate of b_{k-2}, the ISI due to b_{k-1} and b_{k-2} is eliminated. The new differential phase angle $\Delta U_{k,d}^2$ equals

$$\Delta U_{k,d}^2 = b_{k+1} U_{-1}^2 + b_k U_0^2 = b_{k+1} \frac{\pi}{8} + b_k \frac{3\pi}{8} \tag{31}$$

Since $-\pi/2 \leq \Delta U_{k,d}^2 \leq \pi/2$ and the decision threshold is the X-axis, we have to introduce an additional $\pi/2$ phase shift at the $2T$ delay arm in order to observe at the output $\sin(\Delta U_{k,d}^2)$. Consequently the new overall phase

shift χ_2, which includes $\theta_2 = \pi/2$, is

$$\chi_2 = \frac{\pi}{2} + \hat{b}_{k-1}U_1^2 + \hat{b}_{k-2}U_2^2$$

$$= \frac{\pi}{2} + \hat{b}_{k-1}\frac{3\pi}{8} + \hat{b}_{k-2}\frac{\pi}{8} \quad (32)$$

The phase states, after applying these decision feedback phase shifts, are shown in Fig. 6. Notice that the resulting phase states are symmetric and their minimum separation has increased from 45° to 90°, as was the case for the conventional 2-bit differential detector. The decision rule for this 2-bit differential detector with feedback is

$$\hat{a}_k = \text{sgn}\,[d'_2(kT)]$$

where the signal $d'_2(kT)$ includes the additional phase shift χ_2.

One other interesting point is that the shifting rule which was introduced in eqn. 32 is not the only one which produces these improved results. If the signal is phase shifted according to

$$\gamma_2 = (\hat{b}_{k-2} - \hat{b}_{k-1})U_2^2 = (\hat{b}_{k-2} - \hat{b}_{k-1})\frac{\pi}{8} \quad (33)$$

then the phase state diagram illustrated in Fig. 7 results. It is the same diagram as Fig. 6 but $\pm 90°$ phase shifted. Note that both eqns. 32 and 33 will result in exactly the same eye diagram, since $U_1^2 + U_2^2 = \pi/2$. As a matter of fact, by using this identity eqn. 33 can be derived from eqn. 32. By comparing the two relations it can be seen that the second is more suitable for implementation. Thus by manipulating the initial phase shift rules, considerable implementation simplifications can be achieved.

4.3 Decision feedback for the 3-bit differential detector

For the 3-bit detector, the phase shift which should be introduced is

$$\chi_3 = \frac{\pi}{2} + \hat{b}_{k-1}U_1^3 + \hat{b}_{k-2}U_2^3 + \hat{b}_{k-3}U_3^3$$

$$= \frac{\pi}{2} + \hat{b}_{k-1}\frac{\pi}{2} + \hat{b}_{k-2}\frac{3\pi}{8} + \hat{b}_{k-3}\frac{\pi}{8} \quad (34)$$

As in eqns. 28 and 32, the first term of this equation represents the phase shift $\theta_3 = \pi/2$ of eqn. 11. The decision rule associated with eqn. 34 is given by

$$\hat{a}_k = \text{sgn}\,[d'_3(kT)]$$

where $d'_3(kT)$ includes the phase shift χ_3.

A further simplification of eqn. 34 results in

$$\gamma_3 = (\hat{b}_{k-3} - \hat{b}_{k-2})U_3^3 = (\hat{b}_{k-3} - \hat{b}_{k-2})\frac{\pi}{8} \quad (35)$$

The corresponding state-space diagrams are illustrated in Figs. 8 (for eqn. 34) and 9 (for eqn. 35). It is clear from these figures that for both cases the minimum differential phase angle is 90°.

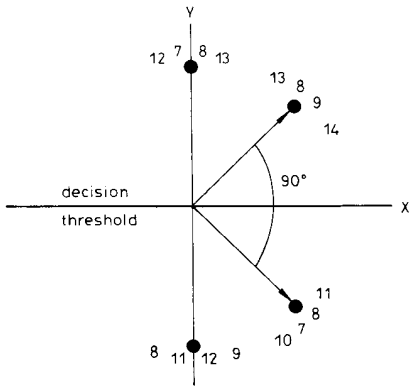

Fig. 6 *Phase-state diagram of the 2-bit differential detector of TFM with decision feedback when the shifting rule of eqn. 32 is being used*
The decision rule for this detector is $\hat{a}_k = \text{sgn}\,[d'_2(kT)]$

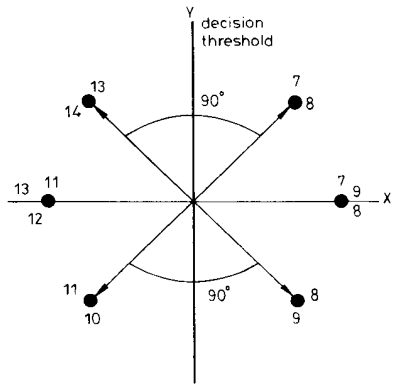

Fig. 7 *Phase-state diagram of the 2-bit differential detector with decision feedback when the shifting rule of eqn. 33 is being used*

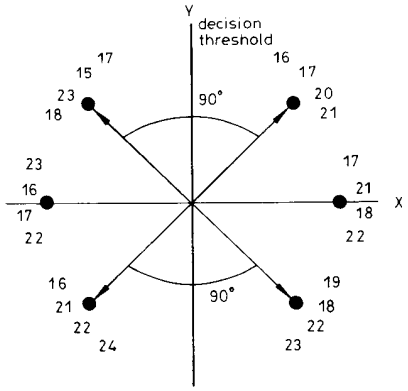

Fig. 8 *Phase-state diagram for the 3-bit differential detector with decision feedback when the shifting rule of eqn. 34 is employed.*
The decision rule for this detector is $\hat{a}_k = \text{sgn}\,[d'_3(kT)]$

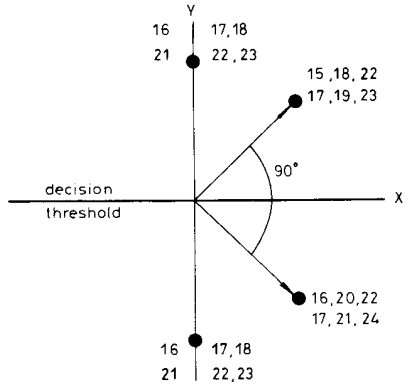

Fig. 9 *Phase-state diagram for the 3-bit differential detector with decision feedback when the shifting rule of eqn. 35 is employed*

4.4 Decision feedback for the m-bit differential detector

For the general case of the m-bit differential detector, the shifting rule is

$$\chi_m = \frac{\pi}{2} + \sum_{j=1}^{n} \hat{b}_{k-j} U_j^m \tag{36}$$

It should be mentioned, however, that for most cases the specific correlative encoding rules of a particular system given by eqn. 2 may significantly simplify eqn. 36.

5 Multiple differential detectors combining and BER performance evaluation results

In order to further improve the performance, the outputs of multiple differential detectors which employ the decision feedback scheme will be jointly utilised. An optimal (e.g. using the maximum likelihood ratio test, MLRT [13]) utilisation of at least two of these differential detectors' outputs results in a nonlinear and therefore generally complex receiver structure [14]. A linear, reduced complexity suboptimal receiver will result by employing as decision law the following relation:

$$\hat{a}_k = \text{sgn}\left[\sum_{m=1}^{M} \rho_m d'_m(kT)\right] \tag{37}$$

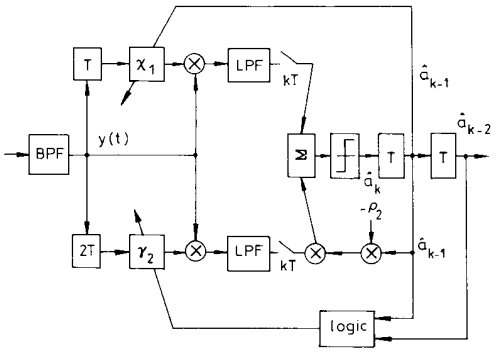

Fig. 10 *Block diagram of the receiver 1 + 2DF which utilises the 1- and 2-bit differential detectors in a decision feedback structure*

The $d'_m(kT)$ represent the sampled outputs of the m-bit detector after decision feedback, ρ_m are combining coefficients, and M is the maximum order of differential detectors used.

For comparison purposes [1], here we shall examine two of these receivers. For the first one, the decision feedback is applied to the 1-bit and 2-bit differential detectors. Then the outputs of these detectors are combined. This receiver will be denoted by $1 + 2DF$, and thus the decision law to be applied here is

$$\hat{a}_k = \text{sgn}\,[d'_1(kT) + \rho_2 d'_2(kT)] \tag{38}$$

However, if instead of the phase shift rule of eqn. 32 we use eqn. 33, the following decision law should be applied:

$$\hat{a}_k = \text{sgn}\,[d'_1(kT) - \rho_2 \hat{a}_{k-1} d'_2(kT)] \tag{39}$$

The appearance of the $-\hat{a}_{k-1}$ in the combining process is due to the fact that the shifting of the signal $d'_2(kT)$ by $\pi/2$ rad is equivalent to the multiplication of the output of the detector by $-\hat{a}_{k-1}$. Notice that, similarly to [1], the transmitter corresponding to the $1 + 2DF$ receiver does not require a differential encoder.

The second receiver configuration we evaluated utilises the 2- and 3-bit differential detectors. By applying the rule described by eqn. 37, its decision law is found to be

$$\hat{a}_k = \text{sgn}\,[-\hat{a}_{k-1} d'_2(kT) + \rho_3 \hat{a}_{k-1}\hat{a}_{k-2} d'_3(kT)] \tag{40}$$

By using at the transmitter the differential encoder $b_k = -a_k b_{k-1}$, this equation can be modified as

$$\hat{b}_k = \text{sgn}\,[-\hat{b}_{k-1} d'_2(kT) + \rho_3 \hat{b}_{k-1}\hat{b}_{k-2} d'_3(kT)] \tag{41}$$

and the information sequence $\{\hat{a}_k\}$ can now be recovered from $\{\hat{b}_k\}$ as follows:

$$\hat{a}_k = -\hat{b}_k \hat{b}_{k-1} \tag{42}$$

Multiplying both sides of eqn. 41 with $-\hat{b}_{k-1}$, the following decision rule can be obtained:

$$\hat{a}_k = \text{sgn}\,[d'_2(kT) - \rho_3 \hat{b}_{k-2} d'_3(kT)] \tag{43}$$

This receiver will be denoted as $2 + 3DF$. The structures of the proposed receivers in block diagram form are illustrated in Figs. 10 and 11.

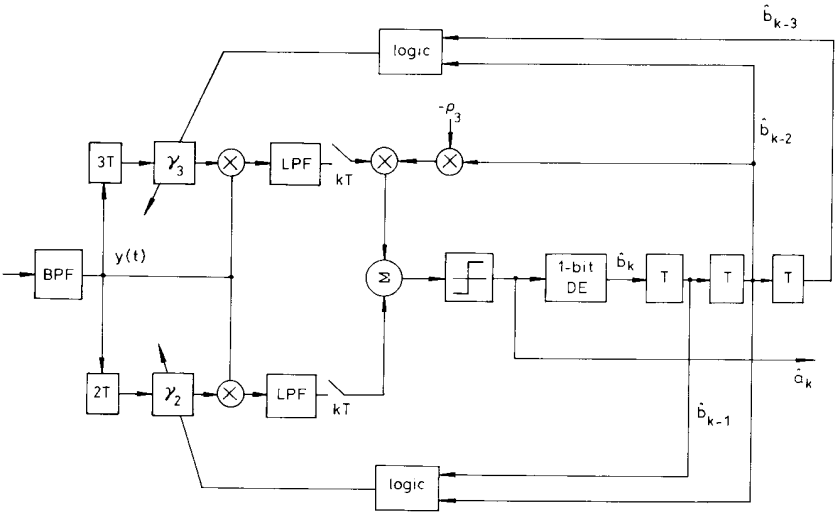

Fig. 11 *Block diagram of the receiver 2 + 3DF which utilises the 2- and 3-bit differential detectors in a decision feedback structure*

In order to evaluate their performance, computer simulation (Monte Carlo error counting techniques) was employed. For comparison purposes the performance of a conventional 2-bit differentially detected TFM scheme was also obtained. The bit error rate (BER) performance evaluation results of the three receivers considered here are plotted for different values of E_b/N_0 (E_b is the bit energy) in Fig. 12. In all three cases for the receiver BPF

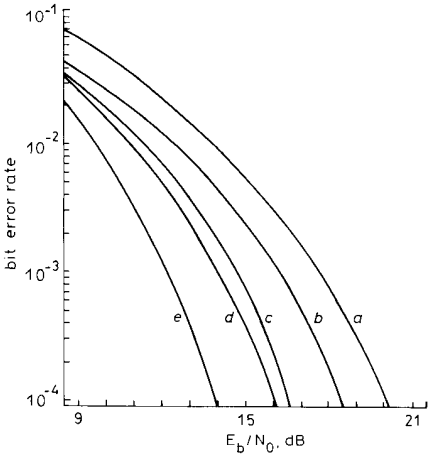

Fig. 12 *Bit error rate (BER) performance evaluation results of the various differential detector schemes for a TFM signal*

a conventional 2-bit differential detector
b bit-by-bit limiter/discriminator detector [8]
c MLSE limiter/discriminator [8]
d 1- and 2-bit differential detector structure (1 + 2DF)
e 2- and 3-bit differential detector structure (2 + 3DF)

a fourth-order Butterworth filter was employed. The performance evaluation results obtained for the TFM scheme indicate that at a BER of 10^{-4} the 1 + 2DF and 2 + 3DF receivers achieve approximately 3.8 and 5.2 dB improvement over the conventional 2-bit differential detector, respectively. The reason why the 2 + 3DF receiver outperforms the equivalent 1 + 2DF receiver is that the combination of a 2- and 3-bit differential detector with decision feedback results in a larger minimum differential phase angle as compared with the equivalent combination of the 1- and 2-bit differential detector. Finally, in Fig. 12 we have included from [8] the performance of a TFM system employing a limiter/discriminator receiver with both bit-by-bit and maximum likelihood sequence estimation (MLSE) detection. It can be seen that both the 1 + 2DF and 2 + 3DF receivers perform better than these limiter/discriminator receivers.

As a closing remark, it is worth pointing out that for other differentially detected CECPM signals, BER performance improvements similar to those reported here for TFM should be expected.

6 Conclusions

New symbol-by-symbol detectors for the differential detection of CECPM signals have been introduced. As a generalisation of the work reported in [1], the proposed detectors use decision feedback to partially remove the destructive effects of ISI which appears at the output of the differential detector. Furthermore, the outputs of more than one differential detector were jointly utilised to further improve the overall BER performance.

As a typical example of the CECPM family of signals, the proposed detection technique has been applied to a TFM scheme. Two receiver structures which jointly employ 1-, 2- and 3-bit differential detectors with decision feedback have been proposed. Performance evaluation results have indicated that gains of up to 5.2 dB (at a BER of 10^{-4}) over a 2-bit conventionally differential detected TFM scheme are possible. As compared with an equivalent TFM scheme employing a limiter/discriminator with MLSE detection [8], the proposed 2 + 3DF receiver offers a gain of more than 2 dB at the same BER.

7 Acknowledgments

We wish to thank Mr. Dimitrios P. Bouras of the Department of Electrical Engineering, University of British Columbia, for his excellent and timely work in drawing the figures for this paper. Useful comments from the three anonymous referees are also acknowledged. This work has been supported in part by the National Sciences and Engineering Research Council (NSERC) of Canada under grant OGP-44312.

8 References

1 YONGACOGLU, A., MAKRAKIS, D., and FEHER, K.: 'Differential detection of GMSK using decision feedback', *IEEE Trans.*, 1988, **COM-36,** pp. 641–649
2 SUNBERG, C.-E.: 'Continuous phase modulation', *Communications Mag.*, 1986, **24,** pp. 25–38
3 MUROTA, K., and HIRADE, K.: 'GMSK modulation for digital mobile radio telephony', *IEEE Trans.*, 1981, **COM-29,** pp. 1044–1050
4 AULIN, T., RYDBECK, N., and SUNBERG, C.-E.: 'Continuous phase modulation. Part II: Partial response signaling', *IEEE Trans.*, 1981, **COM-29,** pp. 210–225
5 MUILWIJK, D.: 'Correlative phase shift keying — a class of constant envelope modulation techniques', *IEEE Trans.*, 1981, **COM-29,** pp. 226–236
6 DESHPANDE, G.S., and WITTKE, P.H.: 'Correlative encoded digital FM', *IEEE Trans.*, 1981, **COM-29,** pp. 156–162
7 DE JAGER, F., and DEKKER, C.B.: 'Tamed frequency modulation, a novel method to achieve spectrum economy in digital transmission', *IEEE Trans.*, 1978, **COM-26,** pp. 534–542
8 CHUNG, K.S.: 'Generalized tamed frequency modulation and its application for mobile radio communication', *IEEE J. Sel. Areas Commun.*, 1984, **SAC-2,** pp. 487–497
9 ANDERSON, J., AULIN, T., and SUNBERG, C.-E.: 'Digital phase modulation' (Plenum, New York, 1986)
10 KOBAYASHI, H.: 'A survey of coding schemes for transmission or recording of digital data', *IEEE Trans.*, 1971, **COM-19,** pp. 1087–1100
11 OGOSE, S., and MUROTA, K.: 'Differential encoded GMSK with 2-bit differential detection', *Trans. IECE Japan*, 1981, **J64-B,** pp. 248–254
12 SIMON, M.K., and WANG, C.C.: 'Differential detection of Gaussian MSK in a mobile radio environment', *IEEE Trans.*, 1984, **VT-33,** pp. 307–320
13 VAN TREES, H.L.: 'Detection estimation and modulation theory, Part I' (Wiley, New York, 1986)
14 MAKRAKIS, D., YONGACOGLU, A., and FEHER, K.: 'Novel receiver structures for systems employing differential detection', *IEEE Trans.*, 1986, **VT-36,** pp. 71–77